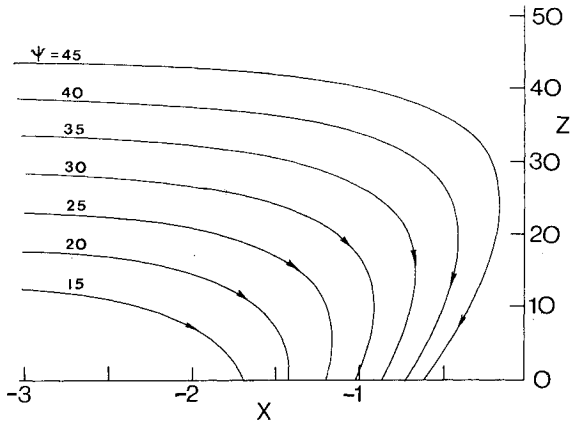

Fig. 1 Streamline pattern for $R=1$, $B=80$, $C=0.05$.

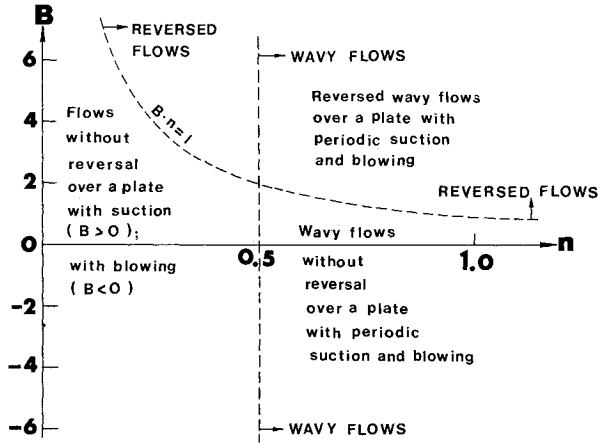

Fig. 2 Exact solutions of the Navier-Stokes equations for flows over a plate, $z=0$, $x<0$.

$$v=-\psi_x=-mB\ \exp(mx-nz) \tag{8}$$

It is seen from Eqs. (7) and (8) that R can be set equal to 1 without loss of generality, since it amounts to rescaling the velocity by a factor of R. It is seen from Eq. (8) that $B>0$ corresponds to suction and $B<0$ corresponds to blowing at the bottom plate, $z=0$. Figure 1 gives the streamlines of the flow for $R=1$, $n=0.05$, and $B=80$. Note the flow reversal due to suction near the trailing edge. It should be pointed out that the flow reversal may not take place when B is sufficiently small.

When $n>0$ but $R^2-4n^2=-q^2<0$, the real part of Eq. (5) yields

$$\psi=Rz+B\exp(Rx/2-nz)\cos qx$$

Hence

$$u=R-nB\exp(Rx/2-nz)\cos qx$$

$$v=-B[(R/2)\cos qx-q\sin qx]\exp(Rx/2-nz)$$

This solution represents the wavy flow over a plate $z=0$, $x<0$ with a periodic variation of suction and blowing along the plate. The possible flows represented by Eqs. (5) and (6), with n real, are delineated in Fig. 2. Note that $R=1$ without loss of generality.

Discussion

A new exact solution of the Navier-Stokes equations is given. The solution can be used to describe the flow with or without flow reversal above a plate with suction and/or blowing. Aside from its own intrinsic interest, it provides us with a simple but exact nonparallel basic flow which could be used for a model analysis of stability of nonparallel flow. The stability analysis of nonparallel flows usually suffers from the uncertainty associated with modeling the nonparallel flows with approximate solutions.

Acknowledgments

This work was supported in part by NASA Research Grant NCC2-280. Thanks are due to Mr. Chen Haibo for his help in producing Fig. 1.

References

[1]Taylor, G. I., "On the Decay of Vorticies in a Viscous Fluid," *Philosophical Magazine*, Vol. 46, 1923, pp. 671-4.

[2]Kovasznay, L.I.G., "Laminar Flow Behind a Two-Dimensional Grid," *Proceedings of the Cambridge Philosophical Society*, Vol. 44, 1948, pp. 58-62.

Effect of a Nearby Solid Surface on a Five-Hole Pressure Probe

Thierry L.B. Tamigniaux* and Gordon C. Oates†
University of Washington, Seattle, Washington

Introduction

HIGH sensitivity and resolution levels have made multiple-hole probes reliable instruments to use in determining rather complex flow situations. In particular, five-hole probes have been used to analyze flow properties of high flow angle regions generated by lift enhancement devices, such as canards, of three-dimensional flows inside compressors and turbines, and of concentric swirling flows inside mixers.

Such probes must be carefully calibrated, however, and calibration usually is carried out in a well-understood uniform stream. When solid boundaries are present, substantial flow realignment can occur with resultant change in measured pressures, so that multiple-hole probes have to be restricted in their use to flows far from containing walls.

In the present investigation, two geometrically similar probes of substantially different scales were first calibrated and then tested in the vicinity of a solid surface. The results provided data on the magnitude of the wall influence and, in addition, indicate, that by including the effect of surface interaction in the calibrating procedure, the range of validity of the results can be slightly extended.

Experimental Procedure

Two probes were used throughout this study. The first probe had an external diameter of 0.158 in., the second had a diameter of 0.6 in. Their geometries were similar in every point (i.e., 45-deg cone angle at the tip and pressure ports located at midspan of the conical surface), except that the pressure ports were not scaled.

Received March 14, 1985; revision received June 21, 1985.
Copyright © American Institute of Aeronautics and Astronautics, Inc., 1985. All rights reserved.

*Graduate Student; presently, Performance Engineer, The Boeing Commercial Airplane Company, Seattle, WA. Member AIAA.

†Professor, Department of Aeronautics and Astronautics, Associate Fellow AIAA.

The first probe was calibrated at a wind tunnel dynamic pressure of $q = 13$ psf (corresponding to a Reynolds number of approximately 9,000), while the second probe was calibrated at $q = 13$ and 1 psf ($Re = 33{,}000$ and 9,000, respectively). Therefore, the two probes could be compared at a similar Reynolds number.

After calibration in a uniform stream, both probes were studied in the proximity of a solid boundary.

The calibration procedure followed was that recommended by Barker et al.[1] Briefly, the procedure involves the measurement of two nondimensionalized pressure coefficients C_α and C_β defined by (see Fig. 1 for the probe geometry and port numbering system)

$$C_\alpha = \frac{p_1 - p_3}{3(p_5 - p_\Sigma/4)}, \qquad C_\beta = \frac{p_2 - p_4}{3(p_5 - p_\Sigma/4)} \tag{1}$$

where $p_1 \rightarrow p_5$ are the pressures measured at the respective port and p_Σ is the sum of p_1 through p_4. The dimensionless velocity components u/V and v/V are then represented as fourth-order polynomials in terms of 15 calibration coefficients and combinations of C_α and C_β (for example, a term in the expression would be $K_n C_\alpha{}^i C_\beta{}^j$, where K_n is the calibration coefficient, i and j integers from 1 to 4, and $0 \le n \le 14$).

Calibration consists of measuring a large number of values of u/V and v/V together with the related values of C_α and C_β. Matrix inversion and a least-squares fit provide the desired calibration coefficients.

This procedure was invoked as follows: for every angle of attack, the sideslip angle was varied manually. A set of seven pressures was taken at every data point. After the sideslip plane was swept, the probe was set to a different angle-of-attack position and the measurements were repeated over the sideslip range. The following flow angles were considered for the small-scale probe:

$\beta = -10, -8, -6, -4, -2, 0, +2, +4, +6$
$+8, +10, +15, +20, +25$, and $+30$ deg
$\alpha = -21, -18, -15, -12, -9, -6, -3, 0, +3,$
$+6, +9, +12, +15, +18$, and $+21$ deg

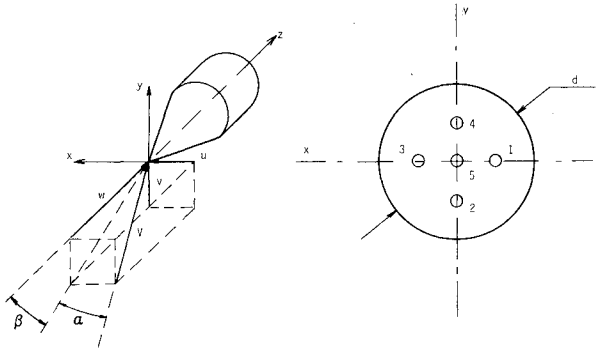

Fig. 1 Coordinate system and probe numbering.

Table 1 Calibration results

	Probe 1, deg $Re = 9{,}000$	Probe 2, deg $Re = 33{,}000$	Probe 2, deg $Re = 9{,}000$
Calibration			
δ_a	0.38	0.58	0.64
δ_β	0.37	0.54	0.61
Position 1 (1,1)			
δ_a	0.68	0.91	1.10
Δ_β	2.86	2.56	3.22
Position 2 (5,2)			
δ_a	0.56	0.56	0.71
Δ_β	1.50	1.21	1.58
Position 3 (9,3)			
δ_a	0.43	0.58	0.78
Δ_β	0.98	0.99	1.29
Position 4 (9,1)			
δ_a	0.72	0.81	0.92
Δ_β	1.98	1.83	1.99

In the case of the large-scale probe, it was found that severe nonlinearities in the calibration appeared for flow angularities in excess of 20 deg. It was decided, therefore, to reduce the calibration space to flow angularities of 20 deg or less, resulting in a calibration space of 12×15 data points.

Following determination of the calibration constants, the flow angles were verified by using the pressures and calibration constants as inputs to obtain the angles as output. The difference between the measured (true) angles and angles computed from the measured pressures (the difference in angle being denoted by δ'_α or δ'_β) was obtained. Typical results showed scatter restricted to 0.5 deg or less.

To facilitate interpretation, the results were least-squares-averaged to give the least-squares angular differences δ_α and δ_β (note that there is no prime for the least-squares value) shown as "Calibration" in Table 1. Considering the wide range of flow angularities considered in the sample, these mean-square errors would seem to be of acceptable accuracy for most investigations. Note that these results are similar to those obtained by Gerner and Maurer.[2]

Flow over a Flat Plate

The probe behavior was then studied in several positions in the vicinity of a flat plate. The probe position was characterized in a two-dimensional coordinate system, the origin of which was located at the flat-plate leading edge. The horizontal distance from the leading edge z was put equal to an integer number m of probe diameters

$$z = m \cdot d$$

Similarly, the vertical distance from the flat plate y was counted in integer numbers n of the probe diameters

$$y = n \cdot d$$

The probe pressure reading behavior was studied in four positions respective of the flat plate corresponding to

$$(m,n) = (1,1); (5,2); (9,3); (9,1)$$

With regard to the plate boundary-layer behavior, the largest Reynolds number experienced is 3×10^5 in the vicinity

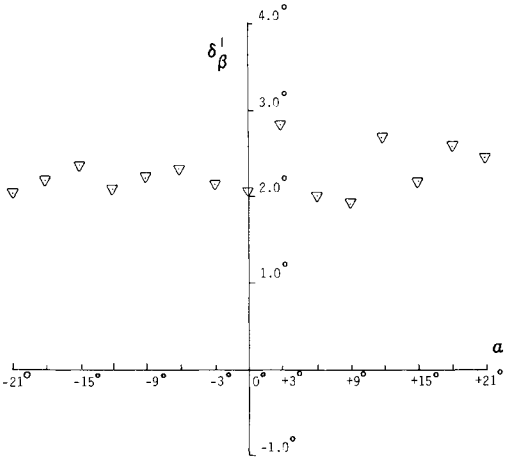

Fig. 2 Difference between true and computed angles of attack for position (1,1).

of position (9,1) when the large probe is used. Hence, the boundary layer should be laminar, and measurements taken with a flattened hypodermic impact probe verified that the boundary-layer width was that expected for a laminar layer. The largest wall interference to be expected is that at station (9,1) with the lowest value of Reynolds number, (8×10^4), which corresponds to a displacement thickness-to-probe-diameter ratio of 0.05, and corresponding flow angularity at the boundary-layer edge of 0.2 deg. These values were taken to be inconsequential in their effect upon the probe readings. The boundary-layer-edge flow angularity at position (1,1) was calculated as 0.5 deg, which could have a measurable but not dominant effect at the probe location. The experimental apparatus used in this part of the experiment was exactly the same as used during the calibration procedure with the addition of the flat plate and its fixture. Once again the true angles were compared to the computed angles.

The sideslip angle behavior was quite similar to that obtained for the case with no sidewall present, with no persistent wall influence becoming evident. In the case of the angle-of-attack behavior, however, although the data scatter was similar to that previously obtained, a substantial and persistent shift in mean angle of attack was found (Fig. 2).

The shift in the mean is termed herein the estimated increment, and denoted by the symbol Δ_β. The least-squares-averaged results for the four probe positions and three probe configurations, as well as the related estimated increments, are shown in Table 1. As is to be expected, the estimated increment in angle of attack decreased with increasing distance from the solid surface. The data reveal that the estimated increment in angle of attack reduces with increased rearward positioning of the probe [compare probes (1,1) and (9,1)]. It appears that this discrepancy is identified with a slight lifting interference caused by the wind tunnel walls above the flat plate introducing slight flow diffusion.

Summary and Conclusions

A calibration method to determine the sideslip angle and angle of attack with five-hole probes was developed and applied to a series of test cases.

The probe behavior was then studied in several positions relative to a flat plate. As expected, the probe overreading of angle of attack increased with increased approach to the wall. The wall interference causes an increased pressure at port 2, which in turn leads to an increase in estimated angle of attack. The estimated increment in angle of attack found in close proximity of the wall substantially exceeded the standard deviation of errors identified with the calibration procedure. From this it is concluded that the validity of probe readings can be extended to within wall influence regimes by including the effect of wall interaction in the calibration procedures. As a rough approximation, the estimated increments obtained in this investigation could be utilized directly in other studies, provided geometric similarity between probes is preserved. It must be noted, however, that this investigation was deliberately conducted to investigate wall influence without the presence of substantial shears. The issue of the effects of boundary layers or separated regions is not addressed.

Acknowledgments

This work was supported by Grant AFOSR-80-0186G from the U.S. Air Force Office of Scientific Research.

References

[1]Barker, K.W., Gallington, R.W., and Minster, S.N., "Calibration of Five-Hole Probe for On-Line Data Reduction," USAFA-TR-79-7.

[2]Gerner, A.A. and Maurer, C.L., "Calibration of Seven-Hole Probes Suitable for High Angles in Subsonic Compressible Flows," AIAA Paper 82-0410, 1982.

[3]Tamigniaux, T.L.B., "An Experimental Investigation of the Wall-Effect on a Five-Hole Pressure Probe," Master of Engineering Thesis, University of Washington, Seattle, March 1984.

Cavity Flow Control for Supersonic Lasers

Wolfgang O. Schall*
DFVLR Institut für Technische Physik
Stuttgart, Federal Republic of Germany

Introduction

BOUNDARY-layer separation in a flow across a deep cavity such as a resonator opening in a flowing gas laser, can be a source of large density inhomogeneities. Producing laser outputs with high-quality beams requires small phase distortions and hence small density variations, $\Delta\rho/\rho$, of the medium. For certain molecular lasers, $\Delta\rho/\rho$ may not exceed 1%. This corresponds to a pressure variation of $\Delta p/p=\gamma\Delta\rho/\rho$ for weak waves in supersonic flows, where γ is the specific heat ratio. Petty et al.[1] and Shen[2] investigated the flowfield of a supersonic duct flow over several cavity shapes. Shen attempted to eliminate flow separation by contouring the edges of the cavity. The importance of edge contours on the achievable beam power in a supersonic CO laser has been confirmed by Schall,[3] who subsequently studied this phenomenon in more detail on resonator cavities.[4]

If a significant reduction of the waves induced by the boundary layer can be achieved, then other applications of cavities in flowing lasers may be possible. For instance, the heat deposited in the cathode sheath of a supersonic discharge laser creates a thickening of the electrode boundary layer, which in turn causes a compression wave of several percent pressure jump at the electrode leading edge.[5] The retraction of the electrodes from the wall into a cavity, together with a suitable shear layer control, could greatly reduce the strength of such waves.[6] In this Note, the effects of controlled variations in cavity gas temperatures and pressures on well-ordered wave strength in the main flow will be reported.

Experimental Studies and Results

A flow channel with a 14.4×25 mm^2 cross section was used in all of the experiments. See Fig. 1. Two openings in the top and bottom wall allowed for the insertion of different edge configurations and cavity designs. The aperture of the cavity opening was fixed at 25×26 mm^2 and the depth of the cavity was held at 40 mm. The sidewalls of the duct were equipped with windows to allow schlieren photography. Based on an estimated wave thickness (order of 10^{-7} m) and a focal length of 0.5 m, the density resolution of the schlieren system was better than 0.5% ($\delta\rho/\rho$), allowing waves from wall steps of $\sim$0.01 mm to be seen. The static pressure was measured at the top wall 40 mm ahead of the center of the cavity opening p_1 and at the cavity wall p_c. Pressure gradients within the cavity were sufficiently small to allow selection of p_c as the characteristic cavity value. For the measurement of pressure profiles across the flow, one window could be replaced by a plate with pressure taps. The pressure resolution was better than 1 mbar (100 Pa) and pressure values of independent runs could be reproduced to within 2.5 mbar. Nitrogen, at a flow rate of 93.5 g/s, was accelerated to Mach number 3.5 at $p_1=100$ mbar. The flow was turbulent with a Reynolds number of 2.5×10^6 and a boundary-layer thickness of 2.75 mm at the cavity leading edge.

Two designs of the edges of the cavity opening were used in the tests. The first was a standard insert with rectangular

Received July 27, 1984; revision submitted March 20, 1985.
Copyright © American Institute of Aeronautics and Astronautics, Inc., 1985. All rights reserved.
*Research Scientist and Groupleader. Member AIAA.